

CONTAMINATION CORRECTION IN SYNPHOT FOR WFPC-2 AND WF/PC-1

S. Baggett, W. Sparks, C. Ritchie, J. MacKenty
February 19, 1996

ABSTRACT

We have implemented a time-dependent photometric calibration of WFPC2 and WF/PC-1 within synphot based on the stellar photometric monitoring data. This provides an empirical correction for the build-up of uniform contaminants on the CCD faceplates of the WFPC2 and WF/PC-1. Although the contaminant issue is less severe for WFPC2, there is more UV science where the effect is still significant. We present the empirical models of the time-variable throughput decline in WFPC2 and WF/PC-1. To activate the correction within synphot, the keyword 'cont#' should be included in the obsmode with the Modified Julian Date as the parameter, e.g: "wfpc2,1,f555w,a2d7,cal,cont#49500.0" or "pc,6,f555w,cal,dn,cont#49219." Note that the automatic pipeline does not include the contamination correction in its computation of the photometric header keywords; the correction must be applied manually by, for example, executing the synphot "bandpar" or "calcphot" tasks off line with the cont# keyword in the obsmode.

1. Introduction.

The presence of contaminants within the WF/PC-1 caused, over time, the build-up of a quasi-uniform layer of material on the cold CCD faceplates of the cameras. This manifested itself by a decline in throughput particularly in the blue, and by an increase in scattering (seen by measuring the light level off the edge of the pyramid). In WFPC-2 great care was taken with the issue of contamination control and indeed the build-up of contaminants is greatly reduced compared to the WF/PC-1. Nevertheless, there is a significant effect because 1) the contaminants affect UV transmission more severely and there is

1. Copies of this report may be obtained from the Science Support Division, Space Telescope Science Institute, 3700 San Martin Drive, Baltimore MD 21218, by e-mail to help@stsci.edu, by anonymous FTP to [stsci.edu](ftp://stsci.edu) directory [instrument_news/WFPC2](ftp://stsci.edu/instrument_news/WFPC2), and by WWW at <http://www.stsci.edu/instruments.html>

much more UV science with WFPC-2 than WF/PC-1 and 2) because the photometric accuracy expected from WFPC-2 is much higher than WF/PC-1 and so even small effects can be relevant.

To quantify the effect, the throughput of the cameras is monitored by taking periodic measurements of a photometric standard star at a variety of wavelengths. The photometric calibration of the cameras, on the other hand, is presented to observers as a fixed set of keywords (provided in the image headers) whose values enable conversion from apparent count rate to an absolute flux level. The keywords are derived using the synphot software package that internally multiplies all relevant throughput curves (OTA, wfpc optics, filters, etc) together for the specific mode of observation and provides as output a flux conversion and characteristic wavelength (PHOTFLAM and PHOTPLAM keywords in the image headers).

These keyword values can also be derived externally to the pipeline using the synphot package which runs under STSDAS. The routine ‘calcband’ provides a tabular version of a throughput curve and the parameters of interest are stored as header keywords (viewable via STSDAS tdump task). To omit the throughput curve generation and only calculate the photometric parameters, the routine ‘bandpar’ may be used; using the specified obsmode (equivalent to the header PHOTMODE keyword), the task computes the response function (uresp = photflam), pivot wavelength, filter bandwidth and more, including the information needed for monochromatic wavelength calibration. Section 4.0 presents examples of these tasks; more details about these tasks and their usage can also be found in the online STSDAS help for each task, the STSDAS manual, and the Synphot Table Update ISR (in preparation).

An enhancement to the synphot software package was the introduction of ‘parameterized’ throughput curves and it is this utility that has enabled us to provide a photometric calibration that is time-dependent, allowing for the contaminant build-up. The current version of the synphot manual available from STScI should be consulted for details of the software and definitions. **Note that the pipeline calwfp/calwp2 routines do not include the “cont” term when defining the obsmode; the contamination correction is currently accessible only by running synphot externally to the pipeline.** That is, the value of PHOTFLAM (used to determine the photometric zeropoint) provided in the header from the automatic pipeline is NOT corrected for contamination. The correction can be applied by executing, for example, the synphot “bandpar” or “calcphot” tasks off line with the cont# keyword in the obsmode.

The intent of the contamination tables is to simplify the empirical correction of observations for contaminant build-up; if preferred, an observer could simply make reference directly to the table of stellar monitor results rather than needing to rely on specific models of the behaviour of the contaminants. To clarify, the synphot adjustment to the flux made by this additional component is on the same system as the stellar monitor data as posted.

In fact, the synphot representation of the time dependence is rather crude (linear interpolation and assumption of fixed wavelength for each filter) and so it may be preferable for some applications to access the monitoring data directly.

2. WFPC2

Observations

From early March 1994 to July 1995, the photometric monitoring proposals obtained images of a spectrophotometric standard star in PC1 and WF3 in the standard wide-band filters before and after each decontamination procedure (decon filter set is F160BW, F170W, F218W, F255W, F336W, F439W, F555W, F675W, F814W). When the nominal target GRW+70D5824 was not visible, the alternate FEIGE 110 was observed. In addition to the decon-related observations, a weekly program executed, imaging GRW+70D5824 in F170W, in all four cameras. As the instrument has proven to be relatively stable from decon to decon, the amount of monitoring has been reduced. As of July 1995, the standard star observations consist of: a single F555W PC image (used for focus monitoring as well), F170W in all four cameras, followed by broadband images in 1 camera (filters: F160BW, F255W, F336W, F439W, F555W, F675W, F814W, and F218W if it fits within the orbit). The series of images, executed before and after each decon, are taken in a different camera each month; in this manner, all four chips will be observed about three times over the course of a year.

The results of the WFPC2 photometric monitoring through ~mid 1994 are detailed in Holtzman et al (1995a, 1995b) and on WWW (tabulated countrates, errors, and MJDs as well as figures; see References for url). To obtain decline rates for the synphot update, data from early 1994 through mid-1995 were used: countrates measured within 0.5" radius apertures were plotted as a function of days after a decon. For completeness, the plots are included at the end of this report along with a list of all WFPC2 decon dates; the fits are discussed in more detail in the next section. Note that after the April 23, 1994 decon, the cameras were cooled from an operating temperature of -76C to -88C. The cooldown was done to minimize the charge transfer efficiency (CTE) problem, from a maximum 10-15% effect down to ~4% effect (Holtzman et al., 1995b). However, operating at the cooler temperature results in more rapid contaminant buildup, so that the photometric throughput declines more rapidly after April 23, 1994. In addition, there was a zeropoint shift, that is, at any given day after a decon, count rates at -76C are systematically lower than those at -88C. The reason for this is not entirely clear, however, for the purpose of updating synphot, we simply include the behavior in the contamination tables as a zeropoint correction. This shift in zeropoint is apparent in Figure 2, where pre-cooldown data has been ratioed to post-cooldown (June 14, 1995) data.

Modelling of the Data

In order to extrapolate the throughput decline to a point just prior to a decontamination and to fill-in gaps in the table, it is necessary to model the photometric monitoring data. The model is used to populate the synphot table; the software will linearly interpolate as needed across wavelength and time. Photometric monitoring data from March 1994 through June 1995 were used to measure decline rates for WFPC2. A simple linear fit was used

$$T = N - (m \cdot t)$$

such that the transmission T declines as a function of days t since a decon. Tables 1 and 2 list the WFPC2 photometric throughput decline rates over 30 days (values of 30m in above eqn.), for the cold and warm operating temperatures, respectively. As noted in Section 2.1, the zeropoints are somewhat lower before the April 23,1994 cooldown; for this reason, normalization $N=1$ is used after the cooldown, and the normalizations (normaliz) listed in Table 2 are used for N prior to the cooldown. For those filters where the decline rate was not measurable (sections marked in grey in the tables), the synphot contamination tables are populated so that no correction is performed for wavelengths in those regions. Until more photometric data becomes available for WF2 and WF4, the contamination tables for these cameras are copies of the WF3 table; WF2 and WF4 corrections are expected to be similar to WF3, to within 1-2%.

Table 1: WFPC2 throughput decline over 30 days (-76C or prior to 4/24/94).²

Filter	PC Loss	Error in Loss	Normaliz	RMS	WF3 Loss	Error in Loss	Normaliz	RMS
F160BW	0.047	0.033	0.865	0.022	0.052	0.051	0.895	0.034
F170W	0.079	0.023	0.910	0.015	0.044	0.022	0.900	0.015
F218W	0.052	0.023	0.931	0.016	0.022	0.027	0.894	0.018
F255W	0.052	0.014	0.920	0.009	0.011	0.041	0.915	0.027
F336W	0.033	0.018	0.969	0.012	0.031	0.019	0.952	0.013
F439W	-0.002	0.006	0.923	0.004	0.000	0.028	0.948	0.018
F555W	-0.016	0.018	0.943	0.012	-0.005	0.013	0.958	0.009
F675W	0.009	0.016	0.976	0.011	0.010	0.009	0.961	0.006
F814W	0.009	0.007	0.996	0.005	-0.014	0.022	0.994	0.015

Table 2: WFPC2 throughput decline over 30 days (-88C or after 4/24/94).³

Filter	PC1 Loss	Error in Loss	RMS	WF3 Loss	Error in Loss	RMS
F160BW	0.271	0.034	0.056	0.388	0.057	0.096
F170W	0.162	0.014	0.024	0.306	0.011	0.018
F218W	0.140	0.010	0.016	0.260	0.012	0.020
F255W	0.070	0.008	0.014	0.142	0.010	0.020
F336W	0.009	0.009	0.015	0.061	0.014	0.023
F439W	-0.001	0.008	0.013	0.025	0.012	0.020
F555W	0.005	0.006	0.010	0.016	0.009	0.015
F675W	0.002	0.006	0.010	0.003	0.007	0.012
F814W	-0.007	0.007	0.011	-0.003	0.009	0.015

3. WF/PC-1

Observations

The WF/PC-1 stellar monitoring program executed with relatively small changes over the duration of the mission. A photometric standard (BD+75D3255) was observed monthly from May 1991 through mission end in Nov 1993, using WF2 and PC6 with filters F230W, F284W, F336W, F439W, F555W, and F785LP (and less frequently, F194W). The 1991/1992 results of the WF/PC-1 monitoring program are described in MacKenty and Ritchie (ISR 93-02); results for 1991 through mission end in Nov 1993 are available in the form of tabulated count rates (apertures of 30 pixel radius for WF2 and 60 pixel radius for PC6), errors, and MJDs for each camera/filter combination used (on WWW) and as a plot of normalized countrates over time (included at the end of this report). **The WF/PC-1 stellar monitor data (not deltaflat corrected) are normalized to the measurements made on day 36 of 1992, which was a couple of days after a decon and does not represent an absolutely clean camera.** However, rather than attempt to provide a calibration for an absolutely clean camera in this case, we will adopt a calibration consistent with the normalization of the stellar monitor data.

2. Loss is measure over 30 days. Areas shaded in grey indicate filters for which 0% decline and/or normalization N=1 were implemented in synphot contamination tables.

3. Areas shaded in grey indicate filters for which 0 decline was implemented in synphot contamination tables.

Modelling of the Data

Since the photometric throughput decline for WF/PC-1 is much larger than for WFPC2, various empirical models for the decline were investigated. An exponential fall-off in throughput with time would be the simplest analytical form that might reasonably be expected for a uniform build-up: if the accumulation rate is uniform and the light loss per unit thickness is constant, then an exponential results. However, in practice this is not a good description of the data. As time progresses, the rate of throughput decline slows down with respect to the initial growth. This could be due, in principle, to 1) a non-uniform accumulation rate, for example if the decontamination itself produced a burst of outgassing or if the reservoir of contaminants started to be exhausted, or 2) the optics of the build-up of the interface layer. For very thin layers comparable to or less than the wavelengths of light involved the transmission properties are non-trivial, and even for thicker layers, much of the modification to the incoming beam takes place at interfaces and not uniformly throughout the depth of the layer.

The present purposes do not extend to a physical understanding of the time dependent behaviour; we are merely interested in describing it empirically. Consistent with the above types of model we fitted two types of curve to the data for each filter. The first model is a double exponential, with data points less than 100 days from a decontamination and those greater than 100 days fitted separately. The second model fitted to all the data and is a modified exponential with a power-law index. Tables 3 and 4 give the results of these model fits.

The first model is based on a two component exponential, where the fit of the log of the transmission versus time is performed separately for time < 100 days and time > 100 days; time is measured in days since last decon. That is, for transmission T , time t , slope m , and intercept i , we fit

$$\log T = i - mt$$

The fits for this model are presented in Table 3.

Table 3: Fits using two-component exponential for WF/PC-1.

Camera	Filter	Slope	Slope Error	Intercept	Intercept Error	RMS
time < 100 days since last decon						
WF2	F194W	0.0243	0.0034	-0.406	0.11	0.226
WF2	F230W	0.01239	0.0007	-0.121	0.038	0.094
WF2	F284W	0.00483	0.0004	-0.059	0.018	0.045
WF2	F336W	0.153e-2	0.18e-3	0.004	0.009	0.023
WF2	F439W	0.59e-3	0.1e-3	-0.004	0.005	0.013
WF2	F555W	0.28e-3	0.8e-4	-0.011	0.004	0.010
WF2	F785LP	no significant slope				
PC6	F194W	0.0198	0.0037	-0.308	0.14	0.267
PC6	F230W	0.0101	0.0007	-0.146	0.033	0.091
PC6	F284W	0.00384	0.0004	-0.0579	0.018	0.046
PC6	F336W	0.00123	0.00022	-0.0215	0.012	0.029
PC6	F439W	0.486e-3	0.16e-3	-0.0024	0.009	0.021
PC6	F555W	0.222e-3	0.897e-4	-0.0055	0.01	0.011
PC6	F785LP	no significant slope				
time > 100 days since last decon						
WF2	F230W	0.0046	0.0011	-0.943	0.2	0.244
WF2	F284W	0.00117	0.28e-3	-0.442	0.05	0.064
WF2	F336W	0.301e-3	0.14e-3	-0.142	0.027	0.033
WF2	F439W	0.792e-4	0.66e-4	-0.068	0.012	0.015
WF2	F555W	0.125e-3	0.30e-4	-0.0359	0.0056	0.007
WFC	F785LP	no significant slope				
PC6	F230W	0.36e-2	0.99e-3	-0.772	0.18	0.225
PC6	F284W	0.95e-3	0.17e-3	-0.342	0.03	0.040
PC6	F336W	0.116e-3	0.98e-4	-0.136	0.018	0.022
PC6	F439W	0.58e-4	0.58e-4	-0.048	0.011	0.013
PC6	F555W	0.71e-4	0.34e-4	-0.026	0.006	0.008
PC6	F785LP	0.56e-4	0.32e-4	0.0047	0.006	0.007

The second model assumes a time dependence of the form

$$T = 10^{[-(t/t_o)^\Gamma]}$$

where transmission is equal to unity at $t=0$. Parameters are derived by fitting a slope and intercept to $\log(1/T) = (\Gamma)(\log t - \log t_0)$, where Γ is the slope and the intercept is $(\Gamma)\log t_0$. Results from fitting with this model are presented in Table 4 below.

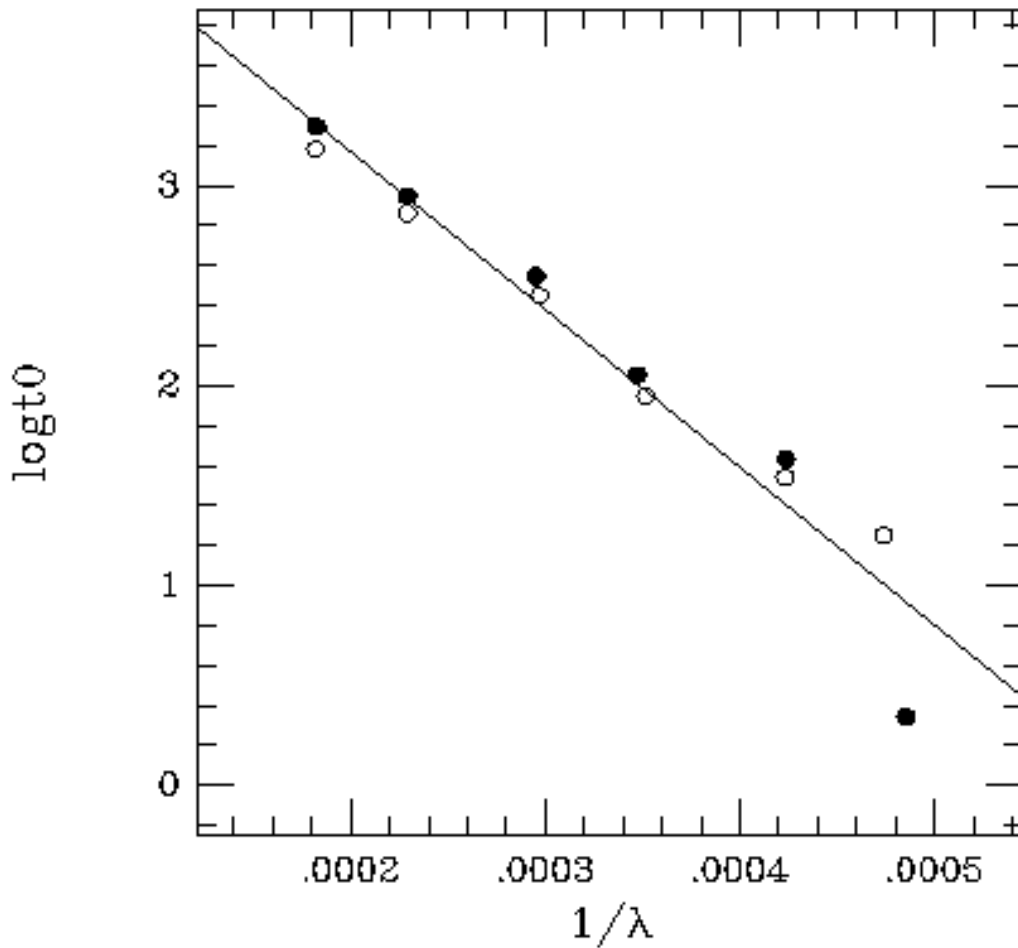
Table 4: Fits using gamma, or modified exponential, model for WF/PC-1.

Camera	Filter	Gamma	Gamma Error	Intercept	Intercept Error	t_0	RMS
WF2	F194W	0.424	0.04	-0.5117	0.053	16.1	0.050
WF2	F230W	0.695	0.022	-1.302	0.041	74.7	0.058
WF2	F284W	0.611	0.026	-1.546	0.049	339.	0.076
WF2	F336W	0.924	0.11	-2.78	0.21	1020.	0.285
WF2	F439W	0.648	0.11	-2.58	0.21	9582.	0.281
WF2	F555W	0.495	0.07	-2.39	0.13	66718.	0.18
WF2	F785LP	indef	indef	indef	indef	indef	indef
PC6	F194W	0.493	0.06	-0.707	0.08	27.2	0.078
PC6	F230W	0.621	0.024	-1.23	0.04	95.6	0.075
PC6	F284W	0.552	0.022	-1.52	0.04	567.	0.064
PC6	F336W	0.535	0.064	-2.00	0.12	5474.	0.17
PC6	F439W	0.466	0.096	-2.31	0.19	90590.	0.23
PC6	F555W	0.558	0.15	-2.71	0.29	71884.	0.37
PC6	F785LP	indef	indef	indef	indef	indef	indef

For the UV data (F194W, F230W, F284W) the modified exponential fits provide the best description of the data while the double exponential worked better for the visual data. Accordingly, the synphot contamination data tables were filled out using these models, with parameters as tabulated.

Although a physical understanding is not required for this empirical description it is still of interest to look at the behaviour of the model parameters. Fig 1 shows that the 100-day e-folding decay rate (i.e. the slope of the first half of the double exponential) follows very closely a linear relationship with inverse wavelength.

Figure 1: E-folding (100 day) Decay Rate



4. Implementation and practical usage

To set up a parametrized throughput table, the monitoring results were re-cast into the appropriate form. Each set of observations (as a function of wavelength) appears as a column in the table, and the parameter (which is part of the column name) is the date of the observation. Since there are gaps in the sequences and since decontamination events introduce discontinuities into the time dependence of the photometric response, it was necessary to model the data and expand the table. Firstly, this was to fill in any gaps with model values, and secondly to provide before and after columns for each decontamination. Each decon has a column associated with a date shortly before and shortly after the procedure; this enables the synphot software to interpolate properly across time (columns) and wavelength (rows). Note that the synphot package only uses linear interpolation and will fail if data are missing, and so this approach ensures a robust and reasonably reliable correction is carried out. For example, a five-column excerpt of the WFPC2 - PC1

contamination table around the time of the June 2,1995 (MJD=49870) decon is shown in the table below.

Table 5. Excerpt from WFPC2-PC1 contamination table “wfpc2_contpc1_005.tab”. The June 1995 decons occurred on the 2nd (MJD=49870.77) and the 27th (MJD=49895.83); column headings are as they appear in the STSDAS table. Note that there is no contamination correction implemented longward of F439W for the PC, as discussed in Section 2.

Column	1	37	38	39
Label	WAVELENGTH	CONT#49870.76	CONT#49870.77	CONT#49895.82
1	500.0	0.75913	1.	0.7741
2	1529.4	0.75913	1.	0.7741
3	1870.7	0.85568	1.	0.86465
4	2203.9	0.87511	1.	0.88287
5	2604.9	0.93774	1.	0.94161
6	3368.0	0.99179	1.	0.9923
7	4316.7	1.	1.	1.
8	5468.0	1.	1.	1.
9	6726.8	1.	1.	1.
10	8009.1	1.	1.	1.
11	11000.0	1.	1.	1.

To use the new component in synphot, include the keyword ‘cont’ and the MJD (modified Julian date) of the observation in the obsmode; the obsmode used in the routine pipeline calibration data is stored in the group parameter PHOTMODE in the science data headers. Examples of the use of the new ‘cont’ keyword, for both WF/PC-1 and WFPC2, are shown below; the command entered in iraf is italicized while the task output is in regular font. MJD is provided in the header keywords EXPSTART and EXPEND or alternatively, the STSDAS task ‘epoch’ can provide MJD:

```
epoch "aug 13,1993:03:00:00pm" qual="" dmy="mdy" printout=mjd,date
13 Aug 1993 15:00:00.00000 FRI
MJD 49212.625000000
```

Using calcphot

For example, for WFPC2, camera 2, without the correction for contamination, the iraf command and output are:

```
calcphot "wfpc2,2,f336w,a2d7,cal" spect=crcalspec$alpha_lyr_001.tab4 form=counts
Mode = band(wfpc2,2,f336w,a2d7,cal)
Pivot Equiv Gaussian
Wavelength FWHM
3358.74 479.4193 band(wfpc2,2,f336w,a2d7,cal)
Spectrum: crcalspec$alpha_lyr_001.tab
VZERO (COUNTS s^-1 hstarea^-1)
0. 5.8070E7
```

4. Note: if you have STSDAS/IRAF and the synphot tables fully installed at your site, the crcalspec should contain the spectra of the HST flux calibration targets/crcalspec points to: /cdbs/calspec/.

The Alpha Lyra spectrum came from the cdb/calspec directories (see Synphot User's Guide, Appendix B, for spectra available from STScI). The same computation, including the contamination correction⁵, is:

```
calcphot "wfpc2,2,f336w,a2d7,cal,cont#49513.0" spect=crcalspec$alpha_lyr_001.tab form=counts
```

```
Mode = band(wfpc2,2,f336w,a2d7,cal,cont#49513.0)
Pivot   Equiv Gaussian
Wavelength   FWHM
3360.444    482.9386  band(wfpc2,2,f336w,a2d7,cal,cont#49513.0)
Spectrum: crcalspec$alpha_lyr_001.tab
VZERO      (COUNTS s^-1 hstarea^-1)
0.         5.5898E7
```

The decline in this example is substantial (5.589E+07/5.807E+07 or ~4%), since MJD=49513 is only three days before a decon procedure⁶.

Similarly, for WF/PC-1, PC6, without and with the correction for contamination:

```
calcphot "pc,6,dn,f439w,cal" spectrum=alpha_lyr_001.tab form=counts
```

```
Mode = band(pc,6,dn,f439w,cal)
Pivot   Equiv Gaussian
Wavelength   FWHM
4355.015    465.5809  band(pc,6,dn,f439w,cal)
Spectrum: crcalspec$alpha_lyr_001.tab
VZERO      (COUNTS s^-1 hstarea^-1)
0.         4.5732E8
```

```
calcphot "pc,6,dn,f439w,cal,cont#49212.0" spect=alpha_lyr_001.tab form=counts
```

```
Mode = band(pc,6,dn,f439w,cal,cont#49212.0)
Pivot   Equiv Gaussian
Wavelength   FWHM
4356.988    465.1969  band(pc,6,dn,f439w,cal,cont#49212.0)
Spectrum: crcalspec$alpha_lyr_001.tab
VZERO      (COUNTS s^-1 hstarea^-1)
0.         4.1800E8
```

Using bandpar and calcband

This section presents examples using the STSDAS tasks bandpar and calcband; as for calcphot, the obsmode can optionally include the "cont#" keyword. Both tasks will compute the photometric parameters photflam (referred to as uresp), pivot wavelength, passband width, peak bandpass throughput, equivalent width, rectangular width, and finally, the equivalent monochromatic flux (along with the reference wavelength and throughput at that wavelength). Calcband will provide the same information as bandpar as well as generate a synthetic passband table of wavelength versus throughput (the online help provides more details). For example, to compute updated photometric keywords for a WFPC2, PC1 observation using F300W and gain 7:

5. Note: obsmode must be enclosed in double quotes to prevent synphot from assuming that the characters to the right of '#' are part of a comment.

6. WFPC2 decontamination dates are tabulated at the end of this report as well as in the regularly updated WFPC2 history file on WWW (see References for url).

```
bandpar obsmode=wfpc2,2,f336w,a2d7,cal photlist=all refwav=undef wavetab=""
# OBSMODE          URESP7      PIVWV    BANDW
wfpc2,2,f336w,a2d7,cal  5.6840E-17    3358.7    203.59
# OBSMODE          TPEAK      EQUVW    RECTW
wfpc2,2,f336w,a2d7,cal  0.0048777    2.2938    470.25
# OBSMODE          EMFLX      REFWAVE  TLAMBDA
wfpc2,2,f336w,a2d7,cal  2.8891E-14    3368.     0.0045127
```

Here, bandpar printed out all the photometric parameters (as set by photlist). No reference wavelength (refwav) was given, so bandpar computes an average wavelength and uses that; if an EMFLX is desired, refwav should be set appropriately. Finally, bandpar was allowed to generate its own default wavelength set to cover the passband wavelength range (as set by wavetab); this will be sufficient for most filters except the narrowbands: for those, smaller wavelength steps are required. The STSDAS task genwave can be used to compute a custom wavelength table, using e.g., 1 angstrom stepsizes:

```
genwave output=mywave minwave=2000. maxwave=10000. dwave=1.
```

Bandpar (and calcband) can then be executed, setting wavetab=mywave.tab. For the calcband example, we use the same obsmode as above,

```
calcband obsmode="wfpc2,2,f336w,a2d7,cal" output=mybandpass wavetab=""
```

The resulting output table is a standard STSDAS binary table; the wavelength and throughput data can be plotted (e.g., using tasks sgraph or plband), printed to an ascii table (tprint), or the photometric keywords, which are stored as table keywords, can be viewed by dumping the table:

```
tdump mybandpass cdfile=STDOUT pfile=STDOUT datafile=STDOUT / page
WAVELENGTH  R      %15.7g angstroms
THROUGHPUT  R      %15.7g ""
GRFTABLE t crcomp$shstgraph_950712a.tab
CMPTABLE t crcomp$shstcomp_950719a.tab
EXPR       t wfpc2,2,f336w,a2d7,cal
APERAREA   r 45238.93
ZEROPT     r -21.1
URESP      r 5.684012E-17
PIVWV      r 3358.74
BANDW      r 203.5902
TPEAK      r 0.004877737
EQUVW      r 2.293758
RECTW      r 470.2504
EMFLX      r 2.889140E-14
           2890. 6.564117E-11
           2893.223 1.905435E-9
...
```

7. The uresp parameter corresponds to the photflam header keyword.

5. Limitations and Future Plans

Indications are that a significant improvement of the photometric quality of the results is achieved by including a contamination correction, particularly in the UV. For WFPC2, the corrections for data taken 30 days after a decon can range from a few percent in the visible to 30-40% in F160BW; uncertainties of these corrections range from 1-3% up to 10% in the UV (Table 2). For WF/PC-1, the corrections for data taken 30 days after a decon ranged from ~5% in the visible to ~40% in F284W and 70% in F230W; the uncertainties in these corrections are 2-3% redward of F336W, about ~5-10% in F336W, F284W, and > 20% in F230W and F194W; Tables 3 and 4). In addition to the fit uncertainties, in order to maintain simplicity of implementation (i.e. so that the stellar monitor data could be used directly as input to the data) we sacrifice some accuracy wherever variations with wavelength are extreme. Another way of thinking of this is that as the contaminant builds up, the effective wavelength of the observation shifts to the red, significantly so in the UV and especially for WF/PC-1. No allowance is made for this effect in the table, and if a more accurate allowance for contaminants is needed, observers are encouraged to extract the data close in time to their observation and to model more carefully the wavelength dependence of the contaminant obscuration.

Furthermore, due to telescope observing time restrictions, only a subset of cameras are normally monitored; for WF/PC-1, this was WF2 and PC6 out of the eight chips. For WFPC2, up until July 1995, two of the four chips, PC1 and WF3, were regularly monitored in the set of wide-band filters, while all four chips are monitored in F170W only. The new Cycle 5 monitoring program obtains observations before and after each decon with a different chip each month, so that all four chips will be observed before and after a decon about three times per year. In addition, Omega Cen images (F336W, F439W, F555W, F675W, and F814W), will be used to evaluate the effects due to position on the chip as well chip-to-chip differences in the throughput decline. Once this data is available, the WF2 and WF4 synphot contamination tables will be updated (as discussed in Section 2, the contamination tables for WF2 and WF4 are currently identical to that in WF3); corrections for WF2 and WF4 are not expected to be more than 1-2% different than corrections for WF3.

Future improvements for the WFPC2 will also include sampling the UV wavelength regime with a variety of standard stars (not just the current white dwarf standard), and using more filters, both wide and narrow bands, in order to better define the contamination behaviour in the UV. And finally, we note that the contamination correction may be implemented in the pipeline in the future; in this case, the results would be stored, if not in the photometric keywords themselves, possibly in header file history records; comments on this idea are welcome and will be solicited before any changes are made. For now, however, the photometric parameters must be derived off-line using the STSDAS synphot software.

6. Summary

We have summarized the synphot time-dependent photometric calibration capability of synphot for WFPC2 and WF/PC-1 data and presented the model fits used to populate the synphot contamination tables. Examples of including the correction in WFPC2 and WF/PC-1 computations are provided as well as a brief discussion of possible limitations to its use.

7.0 Acknowledgements

We thank J. Biretta and B. Whitmore for a critical reading of this manuscript.

8. References

Baggett, S., “WFPC2 SYNPHOT Tables,” photometry memo on WWW (http://www.stsci.edu/ftp/instrument_news/WFPC2/wfpc2_doc.html)

Baggett, S., and Whitmore, B., “WFPC2 History File”, monitoring memo (http://www.stsci.edu/ftp/instrument_news/WFPC2/wfpc2_doc.html)

Baggett, S., Ritchie, C., and Whitmore, B., Synphot Table Updates, Instrument Science Report, in preparation.

Bushouse, H., “STSDAS Synphot User’s Guide,” Version 1.3.3, March 1995. (<http://ra.stsci.edu/STSDAS.html> under Documentation)

Holtzman, J., Hester, J., Casertano, S., Trauger, J., Ballester, G., Burrows, C., Clarke, J., Crisp, D., Gallegher, J., Griffiths, R., Hoessel, J., Mould, J., Scowen, P., Stapelfeldt, K., Watson, A., and Westphal, J., “The Performance and Calibration of the WFPC2”, *PASP* **107**,156 (1995a).

Holtzman, J., Burrows, C., Casertano, S., Hester, J., Trauger, J., Watson, A., Worthey, G., “The Photometric Performance and Calibration of WFPC2” *PASP*, **107**, 1065(1995b).

MacKenty, J., and Ritchie, C., “WF/PC-1 Photometric Monitoring Results”, WF/PC-1 ISR 93-02, Feb 1993.

Ritchie, C., WF/PC-1 Photometric Monitoring Results, a Calibration Memo (http://www.stsci.edu/ftp/instrument_news/WFPC/wfpc1_top.html)

Ritchie, C., WFPC 2 Photometric Monitoring of Standard Star in PC1 and WF3, a Calibration Memo and Figures (http://www.stsci.edu/ftp/instrument_news/WFPC2/wfpc2_doc.html)

Ritchie, C., WFPC 2 Photometric Monitoring of Standard Star in F170W, all chips, a Calibration Memo and Figures (http://www.stsci.edu/ftp/instrument_news/WFPC2/wfpc2_doc.html)

Figure 2: WFPC2 Throughput Monitoring prior to April 23,1994 (-76C)

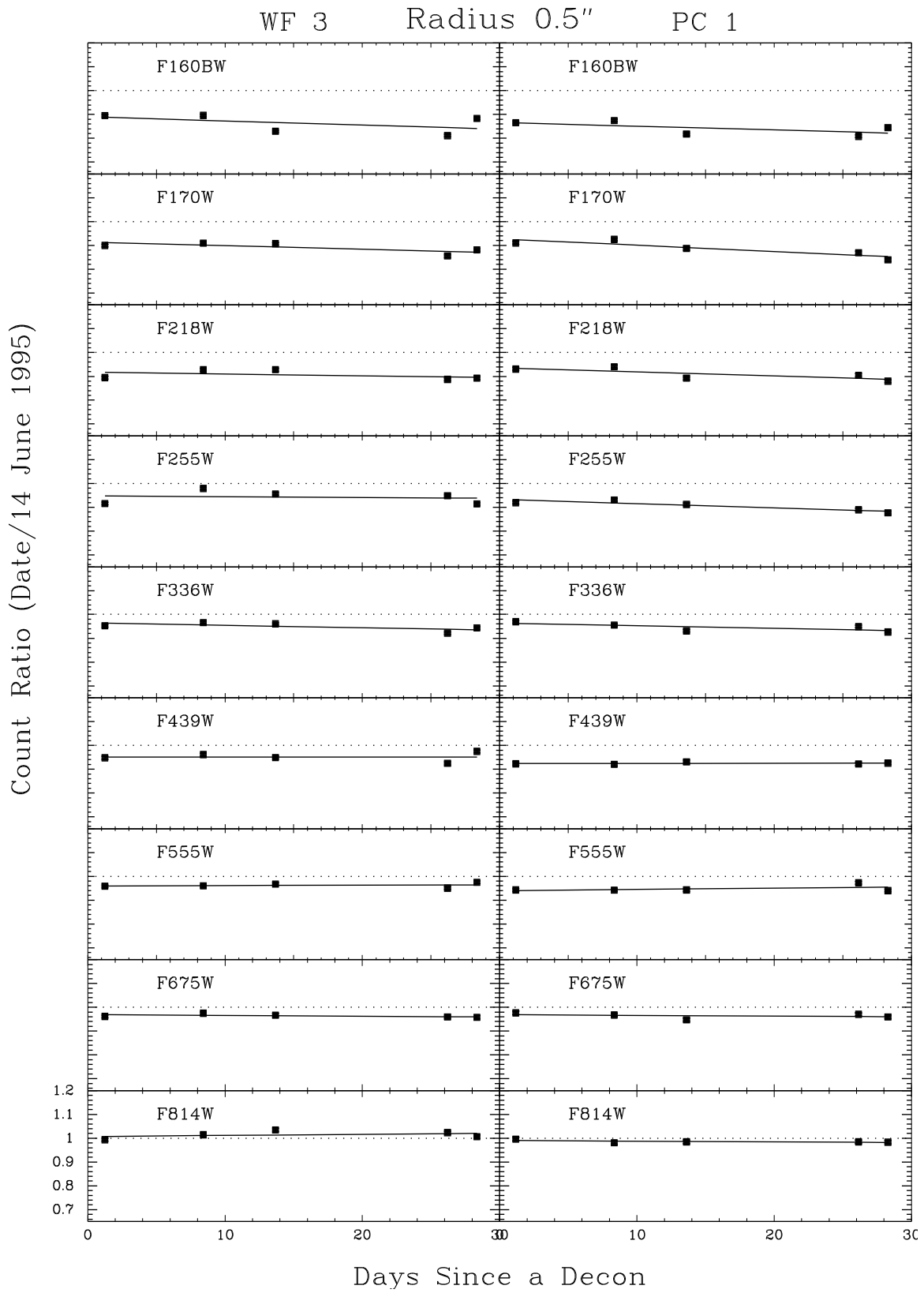


Figure 3: WFPC2 Throughput Monitoring after April 23,1994 (-88C)

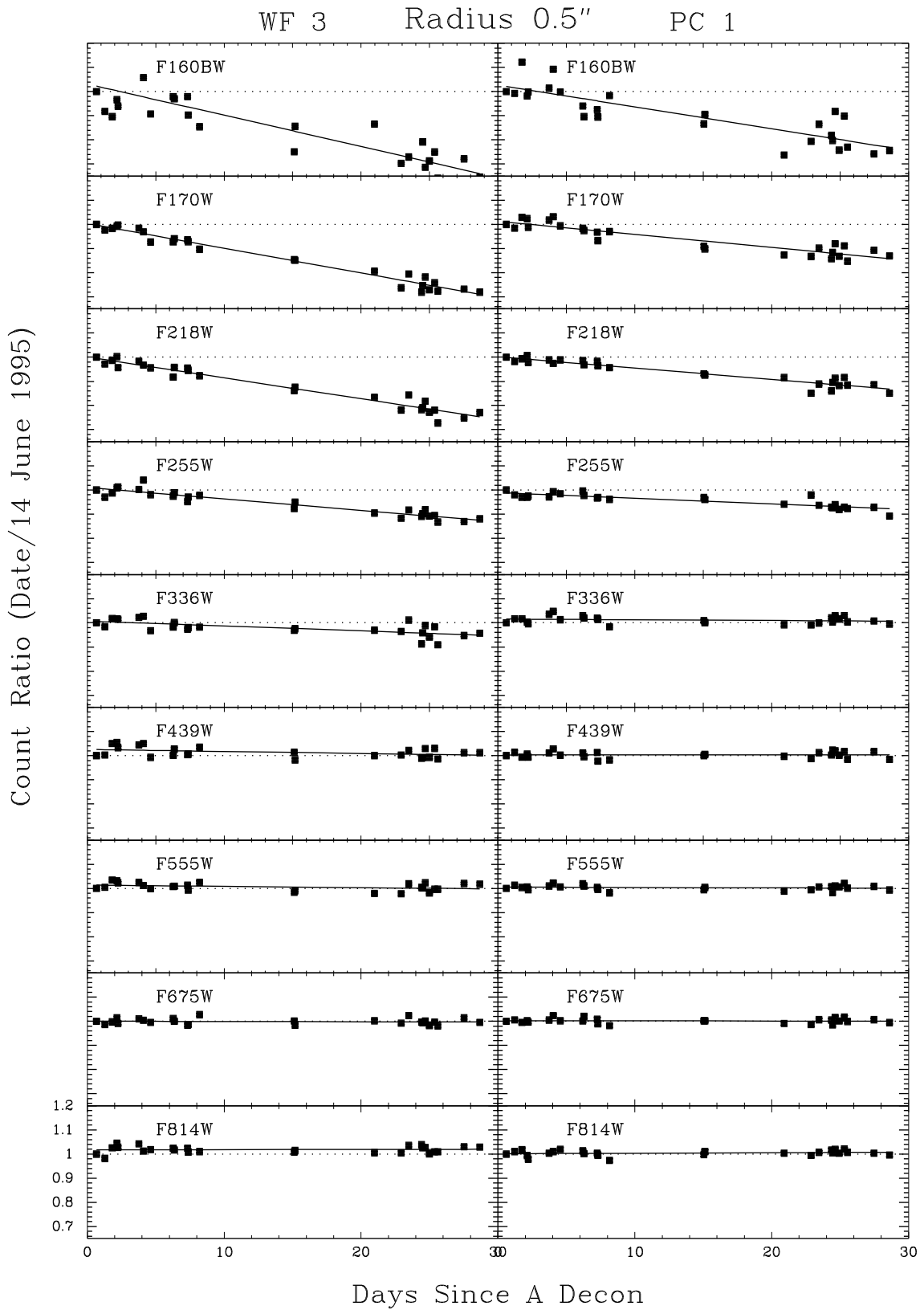
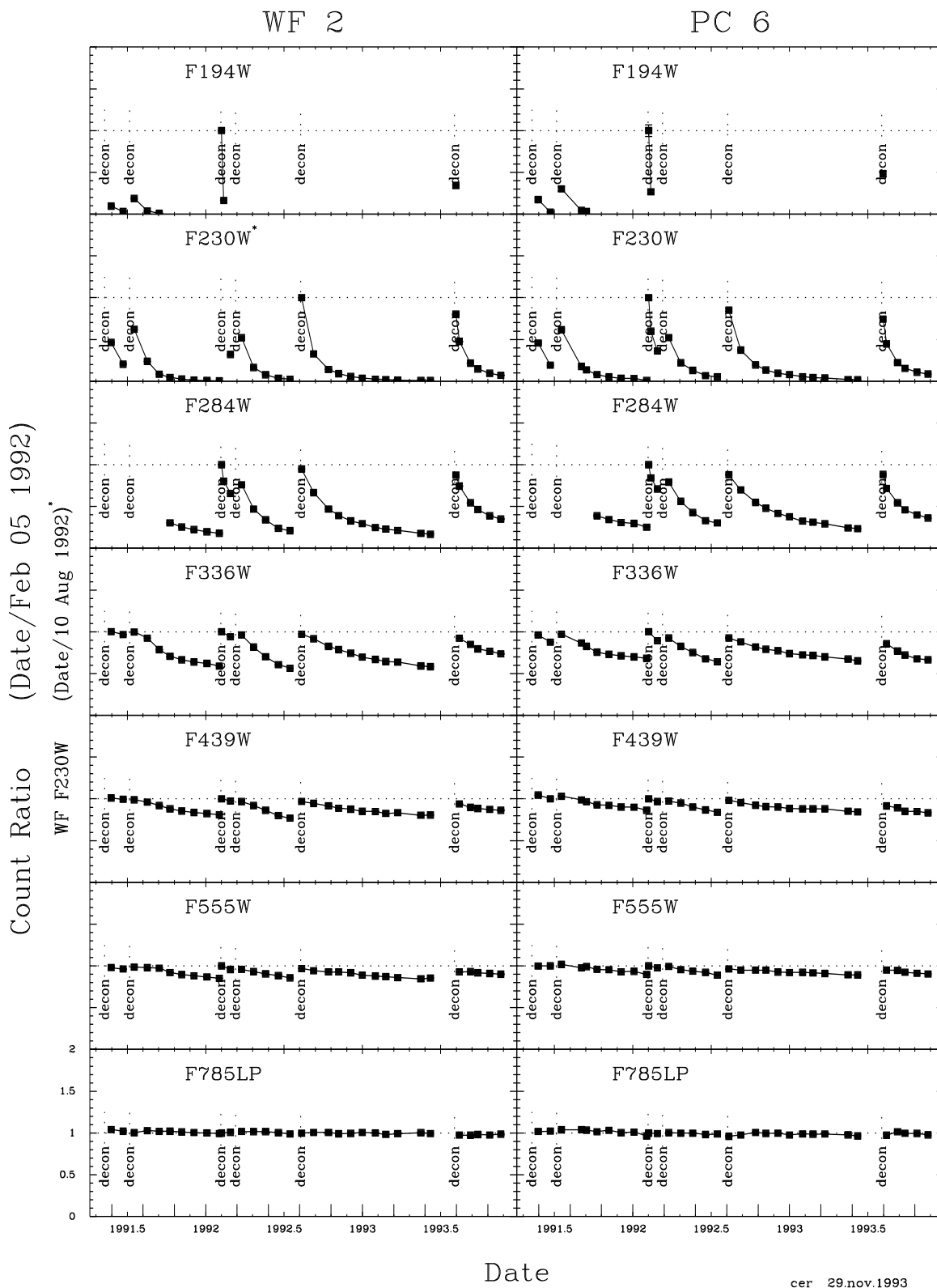


Table 6: Dates of WFPC2 Decontamination Procedures

year	date and time ^a	day of year	modified Julian date	decon length (hours)
1994	22 Feb 11:37	053	49405.4840	6
	24 Mar 11:08	083	49435.4639	6
	24 Apr 00:49	114	49466.0340	6
	23 May 15:00	143	49495.6250	5.5
	13 Jun 11:02	164	49516.4597	12
	10 Jul 11:40	191	49543.4861	12
	28 Jul 07:12	209	49561.3000	12
	27 Aug 09:46	239	49591.4069	12
	25 Sep 00:46	268	49620.0319	12
	21 Oct 00:41	294	49646.0285	12
	19 Nov 17:29	323	49675.7285	6
	18 Dec 06:00	352	49704.2500	6
1995	13 Jan 16:14	013	49730.6764	6
	12 Feb 01:54	043	49760.0792	6
	11 Mar 14:30	070	49787.6042	6
	8 Apr 10:29	098	49815.4368	6
	7 May 01:13	127	49844.0507	6
	2 Jun 18:30	153	49870.7708	6
	27 Jun 20:00	178	49895.8333	6
	30 Jul 08:50	211	49928.3681	6
	27 Aug 05:43	239	49956.2382	6
	22 Sep 03:40	265	49982.1528	6
	17 Oct 09:43	290	50007.4053	6
	15 Nov 08:53	319	50036.3706	6
14 Dec 07:03	348	50065.2929	6	
1996	11 Jan 23:24	011	50093.9750	6
	11 Feb 00:30	042	50124.0208	6

a. Decon starts ~10 hours prior to time listed. Time reflects start of cooldown for 6 hour decon (halfway warmpoint for 12 hour decons). The chips are cold and ready for science about 3.5 hours and 9.5 hours after the time listed, for the 6 and 12 hour decons respectively.

Figure 4: WF/PC-1 Throughput Monitoring



cer 29.nov.1993

Table 7: Dates of WF/PC-1 Decontamination Procedures

year	date and time	day of year	modified Julian date
1991	8 May	128	48384
	5 July	186	48442
1992	3 Feb	034	48655
	4 Feb	035	48656
	3 Mar	063	48684
	8 Mar	068	48689
	7 Aug	220	48841
1993	2 Aug	214	49201